Surface effects on spinodal decomposition in the framework of a linearized theory

H.L. Frisch
Chemistry Department, State University of New York at Albany, 1400 Washington Avenue, Albany, New York 12222 and Institut für Physik, Johannes-Gutenberg-Universität, D-55099 Mainz, Germany*

P. Nielaba and K. Binder
Institut für Physik, Johannes-Gutenberg-Universität, D-55099 Mainz, Germany
(Received 17 February 1995)

Free surfaces of binary mixtures (AB) have a profound effect on phase separation kinetics, since typically one species (say, A) will be preferentially attracted to the surface. Both experiments and numerical simulations have given ample evidence that in the initial stages a (damped) concentration wave forms, in the direction normal to the surface; the amplitude of these concentration oscillations is rapidly damped as one moves into the bulk. We discuss these phenomena in the framework of a linearized theory of spinodal decomposition, where the usual Cahn-type treatment is supplemented by the appropriate boundary conditions. It is shown that the predicted wavelength of the concentration oscillations is compatible with the numerical treatment of the full nonlinear equations. We discuss how these phenomena depend both on the boundary conditions and the bulk state of the mixture to which the quenching experiment leads (temperature, concentration). Extension to thin film geometry and application to experiment are briefly discussed.

PACS number(s): 68.10.−m

I. INTRODUCTION AND OVERVIEW

Recently the effect of surfaces on the kinetics of phase separation in binary systems (AB) has found a lot of attention, both experimentally [1–11] and theoretically [12–18]. The theoretical work, however, is almost entirely of numerical character. While Sagui *et al.* [18] present a Monte Carlo study of a kinetic Ising type model, which hence is a valid description of surface effects in crystalline mixtures, all other work is based on numerical solutions of cell-dynamical type [19] equations. In such a framework, the effect of the surface is described by boundary conditions on the (nonlinear) Cahn-Hilliard-type [20] differential equation. Such boundary conditions have recently been derived either from a continuum approximation to a master equation treatment of a semi-infinite spin-exchange Ising model in mean field equation [21] or—near the critical point of the mixture—from general symmetry considerations [22], and have a nontrivial character. While the qualitative effects of surfaces on phase separation can presumably already be asserted from simplified ad hoc assumptions (as done, e.g., in Ref. [12]) about these boundary effects, for a quantitatively reliable treatment of such phenomena the correct boundary conditions should be used [13,16,17]. Only then can one hope for a quantitative understanding of the interplay between spinodal decomposition and the growth of wetting layers [23].

For spinodal decomposition in the bulk, the linearized

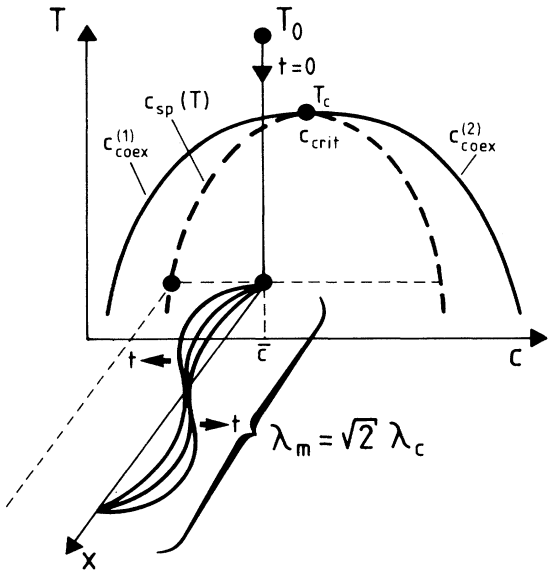

FIG. 1. Schematic description of a quenching experiment that leads to spinodal decomposition of a mixture: one starts at a temperature T_0 such that the system is in thermal equilibrium for times $t < 0$ at the chosen average concentration $\bar{c}$ of one species (say, A). At time $t = 0$, the system is suddenly cooled to a temperature T underneath the coexistence curve (consisting of two branches $c^{(1)}_{coex}$, $c^{(2)}_{coex}$ that merge at a critical point T_c, c_{crit}). If the state point $(\bar{c}, T)$ lies inside of the spinodal curve $c_{sp}(T)$, then the linear theory [20] predicts that in the bulk of the system long wavelength concentration fluctuations (exceeding a critical wavelength λ_c) are unstable, and grow spontaneously in time (maximum growth rate occurs for $\lambda_m = \sqrt{2}\lambda_c$). This is schematically indicated in the figure, where a growth of a single concentration wave in the x direction is shown.

*Permanent address.

theory due to Cahn and Hilliard [20] clearly is a useful first orientation [24–27]; see Fig. 1. Although it is well known that the spinodal curve (where the critical wavelength λ_c in Fig. 1 would diverge [20,24–27]) is an ill-defined concept [24,28–32], except in the mean field limit of long range forces (or equivalent problems such as polymer mixtures with very high molecular weight [30]), the initial length scale $\lambda_m(t=0)$, where the structure factor $S(q,t)$ has its peak $q_m(t)$ [$\lambda_m(t) \equiv 2\pi/q_m(t)$], is estimated roughly correctly, if one is far away from the spinodal. Even for short range systems, where nonlinear effects are important already in the initial stages of phase separation [32–34], the error of the linear theory in predicting $\lambda_m(0)$ is only about 30% [32]. Since many of the experimental systems of interest are polymer mixtures [1–11], where the linear theory is known to be an even better approximation for the very early stages of spinodal decomposition in the bulk [30,31,35,36], we feel there is sufficient interest to consider surface effects in this framework.

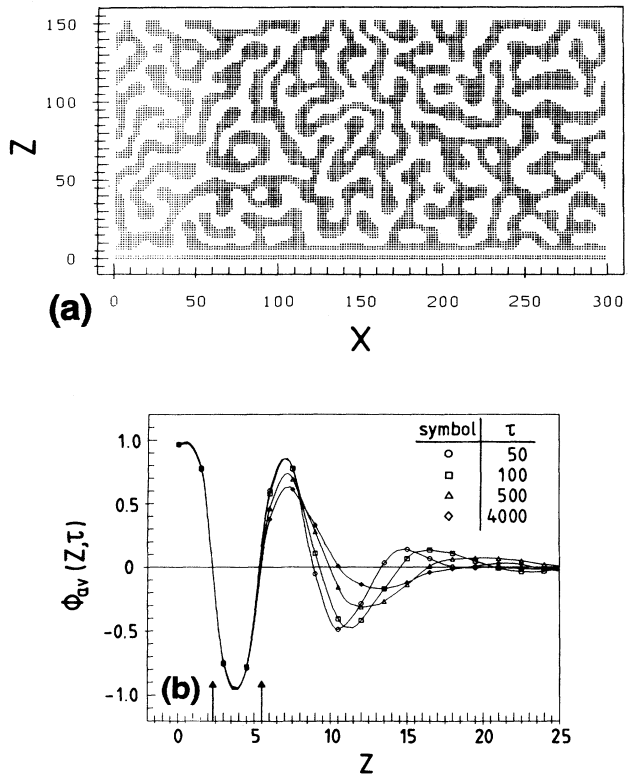

FIG. 2. (a) Snapshot picture of a typical configuration resulting from a discrete implementation of the partial differential equation model with dynamical boundary conditions [Eqs. (1)–(3) below] on a square lattice, using the surface parameters [Eqs. (6)–(15)] $h_1 = 4$, $g = -4$, and $\gamma = 4$ at $z = 0$ (while at $z = 150$ free boundary conditions are used), for a scaled time of $\tau = 500$, after a start from an initial condition corresponding to a critical quench ($\bar{c} = c_{\rm crit}$) from infinite temperature ($T_0 \to \infty$), namely uniformly distributed random fluctuations of amplitude ± 0.025 about a zero background. Species A is represented by black dots, species B is left white. Results are from Puri and Binder [16]. (b) Averaged profiles for the rescaled order parameter $\phi_{\rm av}(Z,\tau)$ as a function of Z (scaled distance from the surface) and τ (scaled time) for the same model as in (a). The averaging is done laterally (in the x direction parallel to the surface) and over an ensemble of five independent initial conditions. Arrows indicate the predictions of the linear theory for the first two zeros of $\phi_{\rm av}(Z,\tau)$ [Eq. (39) below using $\mu_0(s_0') = 1$ in this case]. Numerical results were taken from Ref. [16].

Figure 2 illustrates the type of behavior that we wish to explain here: while in the bulk (i.e., for large scaled distances Z from the wall, $Z \gtrsim 10^1$) the snapshot picture of the configuration shows the typical "seaweed" structure observed for bulk phase separation at critical quenches ($\bar{c} = c_{\rm crit}$, both phases with compositions $c_{\rm coex}^{(1)}$ and $c_{\rm coex}^{(2)}$ in Fig. 1 then have the same volume fraction), at the surface we have an enrichment layer of the A-rich phase, followed by a depletion layer (i.e., a layer of the B-rich phase), while then another A-rich layer follows, which already provides a smooth transition towards the rather different pattern of the bulk. This structure shows up in the variation of the average order parameter $\phi_{\rm av}(z,\tau)$ shown in Fig. 2 (this order parameter here is defined as a rescaled concentration difference, $\phi_{\rm av}(z,\tau) := [c(z,\tau) - c_{\rm crit}]/[c_{\rm coex}^{(2)} - c_{\rm crit}]$: the scaling of time and distance is defined in Sec. II). We see a damped "concentration wave" propagating from the surface towards the bulk, and the picture from the numerical model calculation [13,16] is strikingly similar to corresponding experiments [1]. While the third peak is gradually moving inwards as time proceeds, reflecting the gradual coarsening of the phase separated structures [16,24–27], it is remarkable that the positions and shapes of the first maximum (at the wall) and the adjacent minimum are to a very good approximation *independent of time.* This observation suggests that one should be able to predict these characteristics already from a linearized theory, and the arrows included in Fig. 2(b) show that such an approach indeed is successful.

Having thus motivated our approach, we define our model in Sec. II, while the heart of our calculations is presented in Sec. III, where we obtain the explicit solution of the linear theory of spinodal decomposition with the dynamical boundary condition of Ref. [21]. While Ref. [21] already considered the dynamics of surface enrichment of mixtures in the one phase region at temperatures $T > T_c$, we study here the unstable behavior underneath the spinodal curve. Section IV then summarizes our conclusions and discusses possible applications to experiment.

II. THE MODEL

The microscopic foundation of our description in terms of a lattice model of binary alloys and the corresponding modeling of hopping diffusion in terms of a master equation, which is then used to derive the kinetic equation as well as the boundary condition, has been discussed at length in the literature [16,21]. This discussion will not be repeated here, and we start from Eqs. (46), (47), and (48) proposed by Puri and one of the present authors [16]

for the rescaled concentration deviation $\delta\phi_{k_\parallel}(Z,\tau)$,

$$\frac{\partial}{\partial\tau}\delta\phi_{k_\parallel}(Z,\tau) = \left(k_\parallel^2 - \frac{\partial^2}{\partial Z^2}\right) \times \left(1 - 3\phi_0^2 - \frac{1}{2}k_\parallel^2 + \frac{1}{2}\frac{\partial^2}{\partial Z^2}\right) \times \delta\phi_{k_\parallel}(Z,\tau)\ , \quad (1)$$

supplemented by two boundary conditions at $Z = 0$,

$$\frac{\partial}{\partial\tau}\delta\phi_{k_\parallel}(0,\tau) = h_1 + g\delta\phi_{k_\parallel}(0,\tau) + \gamma\frac{\partial}{\partial Z}\delta\phi_{k_\parallel}(Z,\tau)\Big|_{Z=0} - \left(\frac{\gamma}{4}\right)^{2/3}\frac{\partial^2}{\partial Z^2}\delta\phi_{k_\parallel}(Z,\tau)\Big|_{Z=0} - \frac{5}{6}\left(\frac{\gamma}{4}\right)^{1/3}\frac{\partial^3}{\partial Z^3}\delta\phi_{k_\parallel}(Z,\tau)\Big|_{Z=0} \quad (2)$$

and

$$\frac{\partial}{\partial Z}\left[\delta\phi_{k_\parallel}(Z,\tau) - 3\phi_0^2\delta\phi_{k_\parallel}(Z,\tau)\right]\Big|_{Z=0} + \frac{\partial}{\partial Z}\left[\frac{1}{2}\left(k_\parallel^2 - \frac{\partial^2}{\partial Z^2}\right)\delta\phi_{k_\parallel}(Z,\tau)\right]\Big|_{Z=0} = 0\ . \quad (3)$$

Note that Eq. (1) just results from the standard Ginzburg-Landau-type description of the coarse-grained free energy near T_c: then the order parameter ψ_0 simply is $\psi_0 = \sqrt{3(T_c/T - 1)}$, and $\phi(\vec{R}, Z, \tau)$ is the normalized local order parameter $\psi(\vec{\rho}, z, t)$, where $\vec{\rho}$ is a coordinate parallel to the surface, z is a coordinate perpendicular to it, and $\vec{R}$, and Z are the corresponding rescaled distances

$$\phi(\vec{R}, Z, \tau) = \psi(\vec{\rho}, z, t)/\psi_0,\ Z \equiv z/(2\xi_b),\ \vec{R} \equiv \vec{\rho}/(2\xi_b)\ , \quad (4)$$

and τ is a rescaled time,

$$\tau = (T_c/T - 1)\, t/\left(8\tau_s\xi_b^2\right)\ , \quad (5)$$

where τ_s is the microscopic time constant of the underlying atomistic model (e.g., Kawasaki [37] spin exchange model), and ξ_b is the bulk correlation length. For a hypercubic lattice model with lattice spacing unity and coordination number q considered in [21], we would have $\xi_b = [2q(1 - T/T_c)]^{-1/2}$, but we do assert that Eqs. (1)–(3) should have a more general validity. The average rescaled order parameter ϕ_0 is related to the rescaled concentration difference, of course, $\phi_0 = (\bar{c} - c_{\rm crit})/(c_{\rm coex}^{(2)} - c_{\rm crit})$, and $k_\parallel$ is a momentum coordinate conjugate to $\vec{R}$, $\delta\phi_{k_\parallel}(Z,\tau)$ being a Fourier component of $\delta\phi(\vec{R}, Z, \tau) \equiv \phi(\vec{R}, Z, \tau) - \phi_0$. Equation (1) thus has resulted from linearizing the nonlinear Cahn-Hilliard equation [20] in $\delta\phi$. Being interested in quantities laterally averaged parallel to the surface [Fig. 2(b)] we have to take $k_\parallel = 0$, of course; however, there also may be physical interest in scattering experiments (where the wave vector $\vec{k}_\parallel$ of the scattering must be oriented parallel to the surface, since only then does the system exhibit translational invariance) and thus we consider $k_\parallel \geq 0$ here.

Thus the quantities $\delta\phi_{k_\parallel}(Z,\tau)$ are normalized such that all quantities $(\phi, k_\parallel, Z, \tau)$ are dimensionless, and material constants relating to bulk properties are absorbed in the normalization. The only parameter that remains is the normalized average order parameter ϕ_0; for $\phi_0 = 0$ the quench is called a "critical quench" while otherwise it is "off critical" [24].

Of course, no more freedom is left to eliminate the parameters that describe the physical effects of the surface, and thus parameters h_1, g, and γ remain [Eq. (2)]. Only Eq. (3) does not contain these parameters, since it is simply interpreted as an effect of the conservation law for the concentration: there cannot be any concentration current across the surface at $z = 0$. In brief, the parameters h_1 and g are related (in rescaled form) to the difference in local "effective" chemical potential between species A and B at the surface, and to the (possibly changed) pairwise interactions near the surface [21], if one assumes that the effect of the surface is strictly local. From the theory of wetting phenomena [38] it is well known that long range van der Waals forces (decaying proportional

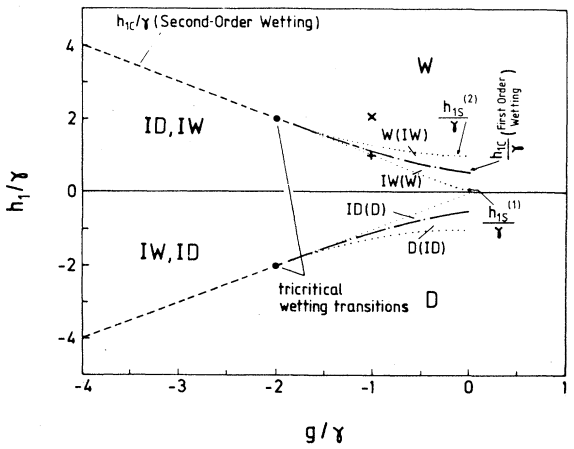

FIG. 3. Phase diagram for the phenomenological model for wetting and drying, Eq. (6). The states are labeled as wet (W), incompletely wet (IW), incompletely dry (ID), and dry (D). Note that the phase diagram is symmetric around the abscissa $h_1/\gamma = 0$ if one interchanges the role of wet and dry states, respectively, due to the symmetry of Eq. (16) against a sign change of ϕ for $h_1 = 0$. For $g/\gamma < -2$ the system has a second-order wetting transition along the line $h_{1c} = -g$ (broken straight line) for $g/\gamma < -2$, which ends at a wetting tricritical point $(g_t/\gamma = -2, h_{1t}/\gamma = 2)$. Dash-dotted curves denote first-order wetting transitions, dotted curves denote "surface spinodals" [stability limits of metastable wet (dry) or incompletely wet (dry) phases, respectively]. The two crosses $(+, \times)$ denote the conditions where the nonlinear equations corresponding to Eqs. (1)–(3) were solved numerically in Ref. [16] and serve for comparison here.

to z^{-3} with the distance from the surface) have profound effects on the surface phase diagram. Since the numerical work [16] has indicated surprisingly little difference in behavior for wet and nonwet regions of the surface, this problem is disregarded here. The parameter γ finally is related to the bulk correlation volume, $\gamma = 4\xi_b^3$, if lengths are measured in units of the underlying lattice spacing. The surface phase diagram depends only on the ratios h_1/γ and g/γ (Fig. 3) but exhibits both second-order and first-order wetting transitions. It can be directly derived from a free energy functional for the semi-infinite system [38–40]

$$\frac{\Delta\mathcal{F}}{k_B T_c} = \int d\vec{R}\left\{\int_0^\infty dZ \frac{1}{2}\left[\frac{1}{2}(\nabla\phi)^2 - \phi^2 + \frac{1}{2}\phi^4\right] - \frac{h_1}{\gamma}\phi_1 - \frac{1}{2}\frac{g}{\gamma}\phi_1^2\right\}, \tag{6}$$

which controls the static equilibrium that results from Eqs. (1)–(3) if there a time-independent solution is sought. Note that in principle Eq. (1) requires four boundary conditions—e.g., if we consider a thin film of thickness D two conditions similar to Eqs. (2) and (3) are also imposed for $Z = D$ [17]—but for a semi-infinite system we rather require that bulk behavior is attained for $Z \to \infty$.

Very close to the bulk critical point one might conclude from Eq. (2) that higher order derivatives in $\partial/\partial Z$ are negligible since then $\gamma \gg 1$. However, already the treatment of the dynamics of surface enrichment [21] has shown that the situation is more subtle and that all terms in Eq. (2) need to be retained in order to derive a physically meaningful solution with the correct limiting behaviors. It is basically through our use of a first-principles boundary condition [21,22] that our treatment differs from related work [14,15].

III. SOLUTION OF THE LINEAR THEORY

For solving Eqs. (1)–(3) it is convenient to use the abbreviations

$$a \equiv 2 - 6\phi_0^2\ , \quad \delta\phi_{k_\parallel}(Z,\tau) = u(Z,t'), \tag{7}$$

where $t' = \tau/2$ and

$$\alpha \equiv k_\parallel^2(a - k_\parallel^2)\ , \quad \beta \equiv 2k_\parallel^2 - a\ . \tag{8}$$

Then Eq. (1) becomes

$$\frac{\partial}{\partial t'}u = \alpha u + \beta\frac{\partial^2 u}{\partial Z^2} - \frac{\partial^4 u}{\partial Z^4}\ , \tag{9}$$

while the boundary conditions, Eqs. (2) and (3), can be combined to give

$$\frac{\partial u(0,t')}{\partial t'} = \frac{h_1}{2} + \frac{g}{2}u(0,t) + \kappa\frac{\partial u(Z,t')}{\partial Z}\bigg|_{Z=0} - \kappa'\frac{\partial^2 u(Z,t')}{\partial Z^2}\bigg|_{Z=0}\ , \tag{10}$$

where abbreviations

$$\kappa = \frac{1}{2}\left[\gamma + \left(\frac{a-\beta}{2}\right)\frac{5}{6}\left(\frac{\gamma}{4}\right)^{1/3}\right], \quad \kappa' = \left(\frac{\gamma}{4}\right)^{2/3} \tag{11}$$

were introduced. The other boundary condition, Eq. (3), reads

$$\frac{a-\beta}{2}\left(\frac{\partial u}{\partial Z}\right)\bigg|_{Z=0} + \left(\frac{\partial^3 u}{\partial Z^3}\right)\bigg|_{Z=0} = 0\ . \tag{12}$$

Using then the Laplace transform

$$\bar{u}(Z,s) = \int_0^\infty \exp(-st')\, u(Z,t')\, dt' \tag{13}$$

we obtain in terms of the initial condition $u(Z,0) = u_0$ $(Z \geq 0)$ that

$$(s-\alpha)\bar{u} - u_0 = \beta\frac{\partial^2\bar{u}}{\partial Z^2} - \frac{\partial^4\bar{u}}{\partial Z^4}\ . \tag{14}$$

The boundary conditions, Eqs. (10) and (12), become

$$s\bar{u}(0,s) - u_0 = \frac{h_1}{2s} + \frac{g}{2}\bar{u}(0,s) + \kappa\frac{\partial\bar{u}(Z,s)}{\partial Z}\bigg|_{Z=0} - \kappa'\frac{\partial^2\bar{u}(Z,s)}{\partial Z^2}\bigg|_{Z=0}\ , \tag{15}$$

$$\frac{a-\beta}{2}\frac{\partial\bar{u}(Z,s)}{\partial Z}\bigg|_{Z=0} + \frac{\partial^3\bar{u}(Z,s)}{\partial Z^3}\bigg|_{Z=0} = 0\ . \tag{16}$$

Setting

$$\bar{u}(Z,s) = \frac{u_0}{s-\alpha} + V(Z,s)\ , \tag{17}$$

Eq. (14) becomes

$$(s-\alpha)V = \beta\frac{\partial^2 V}{\partial Z^2} - \frac{\partial^4 V}{\partial Z^4}\ , \tag{18}$$

while the boundary Eq. (15) is slightly modified to

$$\frac{(\alpha - g/2)u_0}{s-\alpha} - \frac{h_1}{2s} = (g/2 - s)V(0,Z) + \kappa\frac{\partial V(Z,s)}{\partial Z}\bigg|_{Z=0} - \kappa'\frac{\partial^2 V(Z,s)}{\partial Z^2}\bigg|_{Z=0}\ . \tag{19}$$

We now proceed by trying a solution in terms of an oscillatory damped wave,

$$V(Z,s) = e^{-\nu(s)Z}\{A(s)\cos[\mu(s)Z] + B(s)\sin[\mu(s)Z]\}\ . \tag{20}$$

Equations (12), (19), and (20) then imply

$$\Omega^{-1}(s) \equiv A(s)/B(s) = \frac{(a-\beta)\mu/2 + 3\nu^2\mu - \mu^3}{(a-\beta)\nu/2 - 3\nu\mu^2 + \nu^3}, \tag{21}$$

$$\frac{(\alpha - g/2)u_0}{s-\alpha} - \frac{h_1}{2s} = (g/2 - s)A + \kappa\mu B - \kappa\nu A - \kappa'[(\nu^2 - \mu^2)A - 2\nu\mu B] \quad (22)$$

and eliminating $B(s)$ from Eq. (22) with the help of Eq. (21) one further obtains

$$A(s) = \frac{[(\alpha - g/2)/(s-\alpha)]\,u_0 - h_1/2s}{g/2 - s + \kappa\mu\Omega - \kappa\nu - \kappa'\,[(\nu^2 - \mu^2) - 2\nu\mu\Omega]} . \quad (23)$$

At this point we note that Eq. (20) can, of course, also be written in terms of a simple cosine function if we allow for an amplitude $C(s)$ and a phase $\varphi(s)$,

$$V(Z,s) = C(s)\exp[-\nu(s)\,Z]\,\cos[\mu(s)Z - \varphi(s)] , \quad (24)$$

where the phase $\varphi(s)$ is $\varphi(s) = \arctan[\Omega(s)]$ and clearly is fixed by bulk properties only, independent of the constants h_1, g, γ characterizing the surface. The latter quantities do enter the amplitude prefactor $A(s)$ [or $C(s) = \sqrt{A^2(s) + B^2(s)}$, respectively], as expected.

In Eq. (20), the quantity $\nu(s)$ can be interpreted as an inverse frequency-dependent correlation length, while $\mu(s)/2\pi$ is an inverse wavelength. These quantities follow when we require that Eq. (20) solves the bulk equation, Eq. (18); we simply have to equate the coefficients of $\cos(\mu Z)$ and $\sin(\mu Z)$ on both sides to find

$$(s-\alpha) = \beta\,(\nu^2 - 2\nu\mu - \mu^2) + \nu^4 + 4\nu^3\mu + 6\nu^2\mu^2 - 4\nu\mu^3 - \mu^4 , \quad (25)$$

$$(s-\alpha) = \beta\,(\nu^2 + 2\nu\mu - \mu^2) + \nu^4 - 4\nu^3\mu + 6\nu^2\mu^2 + 4\nu\mu^3 - \mu^4 . \quad (26)$$

Subtracting these equations from each other yields

$$0 = -4\beta\nu\mu + 8\nu^3\mu - 8\nu\mu^3 , \quad \nu = \pm\sqrt{\beta/2 + \mu^2} , \quad (27)$$

and substituting this result in Eq. (25) yields a biquadratic equation for μ,

$$6\mu^4 + 4\mu^2\beta + \frac{3}{4}\beta^2 - s + \alpha = 0 , \quad (28)$$

and hence the solutions for the inverse wavelengths $\mu(s)/2\pi$ are

$$\mu_{1,2} = \pm\frac{1}{\sqrt{12}}\sqrt{-4\beta + \sqrt{2}\sqrt{-\beta^2 + 12(s-\alpha)}} , \quad (29)$$

$$\mu_{3,4} = \pm\frac{1}{\sqrt{12}}\sqrt{-4\beta - \sqrt{2}\sqrt{-\beta^2 + 12(s-\alpha)}} . \quad (30)$$

In order to discuss which of these many solutions has to be taken, it is useful to rewrite these functions $\nu^2(s)$ and $\mu^2(s)$ in terms of the physical parameters $k_\parallel$ and ϕ_0:

$$[\mu^2(s)] = \frac{1}{6}\left[4\left(1 - k_\parallel^2 - 3\phi_0^2\right) \pm \sqrt{2}\sqrt{-1 - 4k_\parallel^2 + 2k_\parallel^4 + 6\phi_0^2 + 12k_\parallel^2\phi_0^2 - 9\phi_0^4 + 3s}\,\right] , \quad (31)$$

$$[\nu^2(s)] = \frac{1}{6}\left[-2\left(1 - k_\parallel^2 - 3\phi_0^2\right) \pm \sqrt{2}\sqrt{-1 - 4k_\parallel^2 + 2k_\parallel^4 + 6\phi_0^2 + 12k_\parallel^2\phi_0^2 - 9\phi_0^4 + 3s}\,\right] . \quad (32)$$

Since we wish that for $Z \to \infty$ we recover the standard behavior of the bulk, which is simply given by the first term on the right-hand side of Eq. (17) [using Eq. (13) we see that this yields the usual concentration wave growing with time], $V(Z,s)$ must decay to zero for $Z \to \infty$. Hence we must choose only the positive solution in Eq. (27). In addition, the negative signs in Eqs. (29) and (30) are redundant: $\cos(\mu Z)$ is an even function of its argument; while the function $\sin(\mu Z)$ is odd, $\Omega(s)$ also changes sign when μ changes sign, and hence the minus signs in Eqs. (29) and (30) do not yield anything new.

A further obvious condition that we must require is that $\mu(s)$ is real-valued. From Eqs. (29)–(32) we see that the expression underneath the square root in Eqs. (31) and (32) must be non-negative, which yields

$$s \geq s_0 \equiv \frac{1}{3}\left[\left(1 - 3\phi_0^2\right)^2 - 2k_\parallel^4 + 4k_\parallel^2\left(1 - 3\phi_0^2\right)\right] . \quad (33)$$

Considering wavelengths and states inside the spinodal we have $-\beta/2 = 1 - k_\parallel^2 - 3\phi_0^2 > 0$. Then Eq. (33) ensures that $\mu^2(s) > 0$ if the + sign in this equation is taken. The condition that $\nu^2(s) > 0$, however, excludes the minus sign in Eqs. (31) and (32), and hence the solution Eq. (30), where this sign comes from, has to be discarded altogether. In fact, even if the plus sign in Eqs. (31) and (32) is taken, the condition $\nu^2(s) > 0$ yields an additional constraint on the frequency, namely,

$$s \geq s_0' = \left(1 - 3\phi_0^2\right)^2 . \quad (34)$$

One can show that no exponentially decaying solution of the type of Eq. (20) exists for small s and $k_\parallel = 0$. The conditions Eqs. (33) and (34) have to be taken into account when one transforms back from the frequency domain to the time domain. Since the resulting integrals are clumsy and not analytically soluble, we avoid this step here altogether and rather discuss only the general features of the Laplace transform $\bar{u}(Z,s)$ or its surface-directed part $V(Z,s)$ here.

Let us first ask where this function has its zeros and its extrema: the zeros $Z = Z_0(s)$ are solutions of

$$\cos[\mu(s)Z_0(s)] + \Omega(s)\sin[\mu(s)Z_0(s)] = 0 ,$$

$$Z_0(s) = -\frac{1}{\mu(s)}\arctan[1/\Omega(s)] . \quad (35)$$

The maxima and minima are at $Z = Z_m$, satisfying

$$[\mu(s)\Omega(s) - \nu(s)]\cos[\mu(s)Z_m(s)]$$

or

$$= [\mu(s) + \nu(s)\Omega(s)]\sin[\mu(s)Z_m(s)] , \quad (36)$$

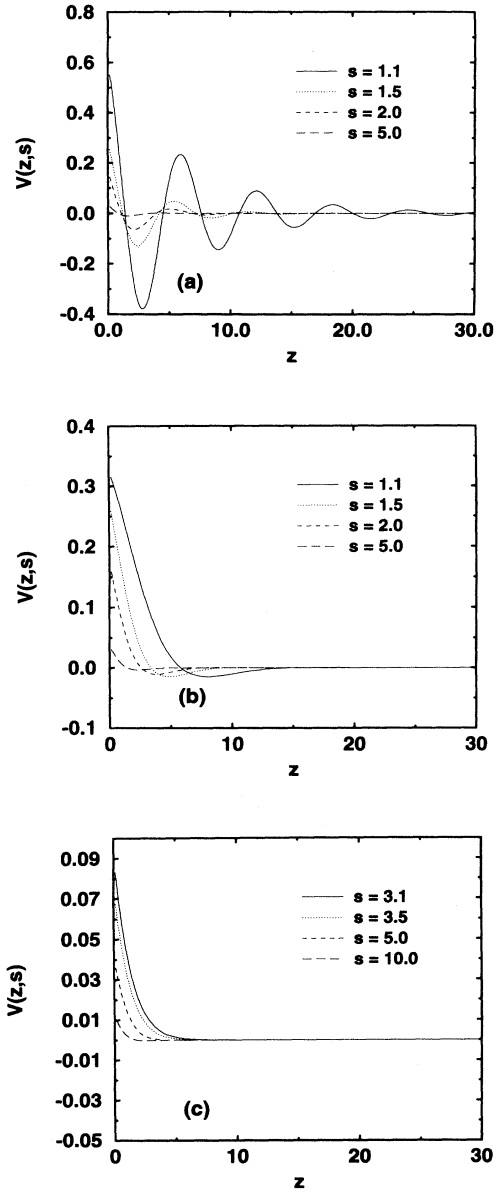

FIG. 4. Surface part $V(Z,s)$ of the Laplace transform $\bar{u}(Z,s)$ plotted vs the scaled distance Z for the case $h_1 = 4$, $\gamma = 4$, $g = -4$, amplitude $u_0 = 0.025$, $\phi_0 = 0$, and three values of the scaled wave number $k_\parallel$: $k_\parallel = 0$ (a), $k_\parallel = 1$ (b), and $k_\parallel = \sqrt{2}$ (c). In each case, four values of the scaled frequency s are shown, as indicated in the figure. Note that the frequency limit $s_0' = 1$ here, while $s_0 = 1/3$ (a), 1 (b), and 1/3 (c).

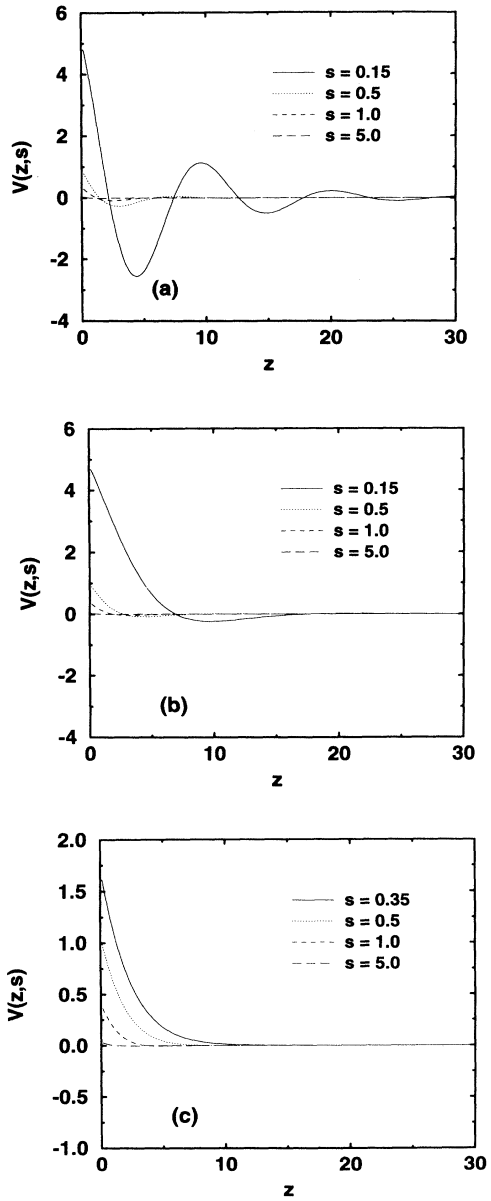

FIG. 5. Surface part $V(Z,s)$ of the Laplace transform $\bar{u}(Z,s)$ plotted vs the scaled distance Z for the case $h_1 = 4$, $\gamma = 4$, $g = -4$, amplitude $u_0 = 0.025$, $\phi_0 = 0.47$, and three values of the scaled wave number $k_\parallel$: $k_\parallel = 0$ (a), $k_\parallel = \sqrt{1 - 3\phi_0^2}$ (b), and $k_\parallel = \sqrt{2}\sqrt{1 - 3\phi_0^2}$ (c). In each case, four values of the scaled frequency s are shown, as indicated in the figure.

$$\tan[\mu(s)Z_m(s)] = \frac{\mu(s)\Omega(s) - \nu(s)}{\mu(s) + \nu(s)\Omega(s)} . \qquad (37)$$

We emphasize that neither $Z_0(s)$ nor $Z_m(s)$ depend on the surface parameters h_1, g, and γ. From Eq. (37) we recognize that an extremum always will occur close to the surface, $Z_m(s) = 0$, if $\mu(s), \nu(s) \ll (a-\beta)/2 = 4(1 - k_\parallel^2/2 - 3\phi_0^2)$, because then in Eq. (21) the terms nonlinear in μ or ν can be neglected and $\Omega(s) \approx \nu(s)/\mu(s)$. From Eqs. (31) and (32) we see that for $k_\parallel \to 0$ and s near s_0' this condition is roughly obeyed if ϕ_0 is small, since then $\mu(s) \approx \sqrt{1 - 3\phi_0^2}$, nearly independent of s, and $\nu(s) \approx 0$. In this limit, $\Omega(s)$ clearly is very small, and then the

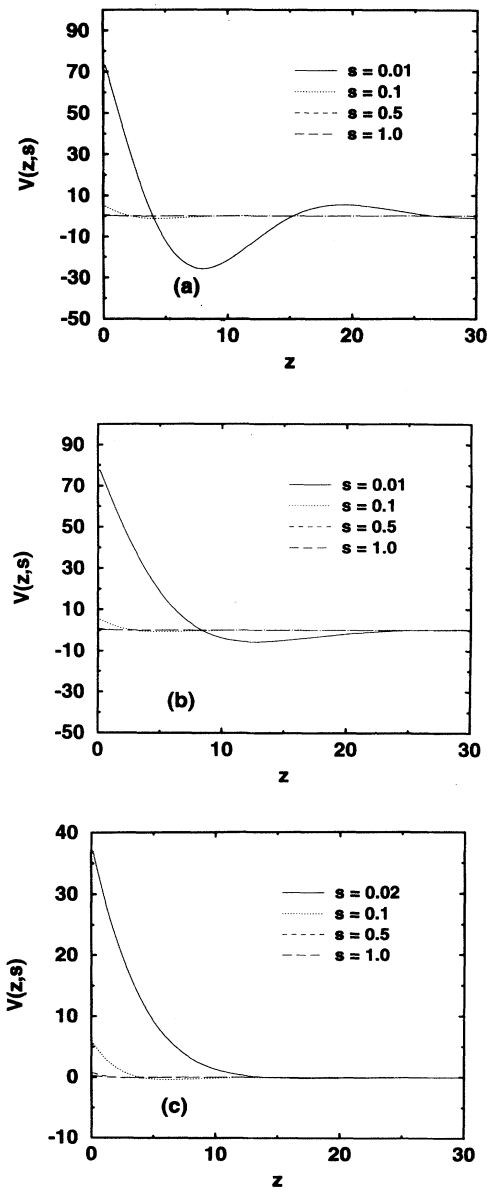

FIG. 6. Same as Fig. 5 but for $\phi_0 = 0.56$.

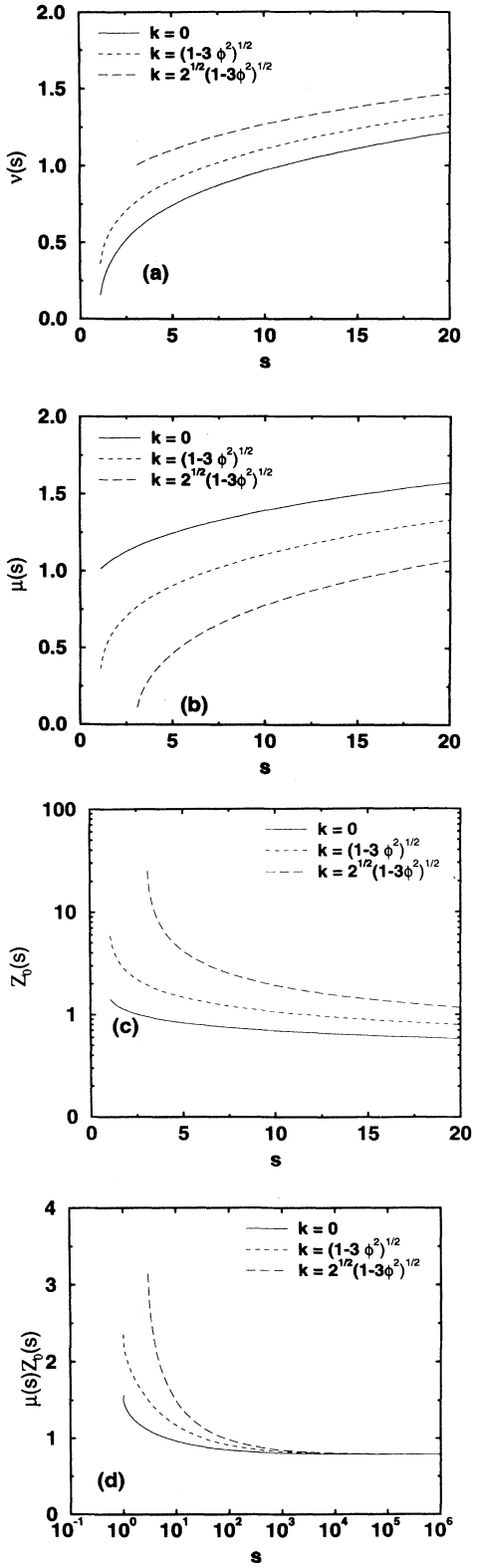

FIG. 7. Inverse frequency dependent correlation length $\nu(s)$ (a), inverse wavelength $\mu(s)$ (b), scaled position of the first zero $Z_0(s)$ (c), and the product $\mu(s)Z_0(s)$ (d) for $\phi_0 = 0$ plotted vs scaled frequency s for three choices of $k_\parallel$, as indicated in the figure.

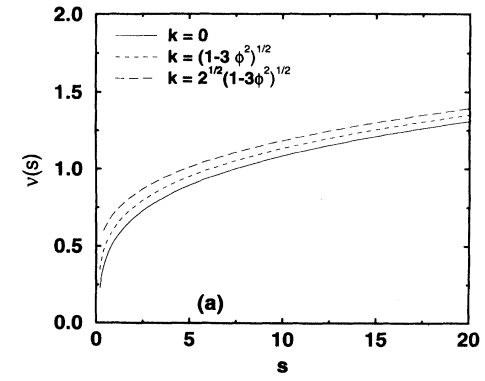

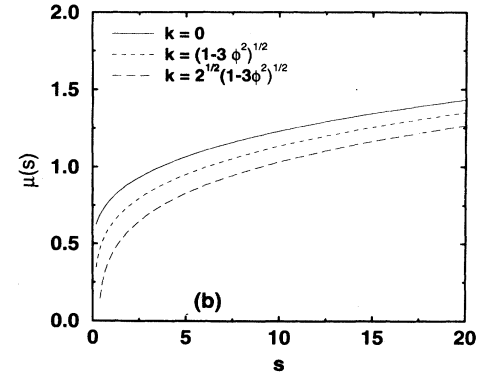

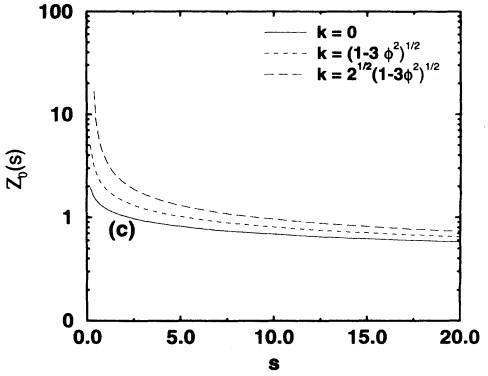

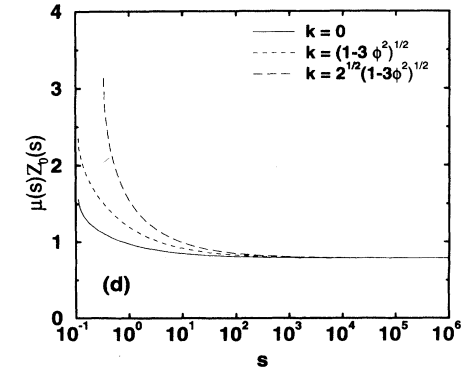

FIG. 8. Same as Fig. 7 but for $\phi_0 = 0.47$.

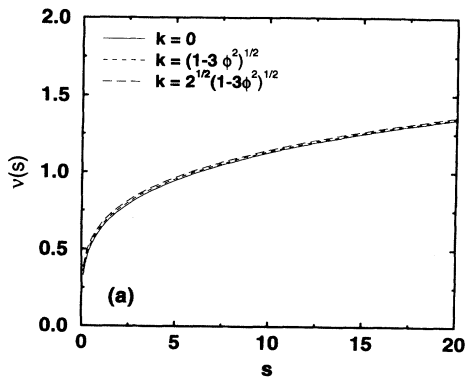

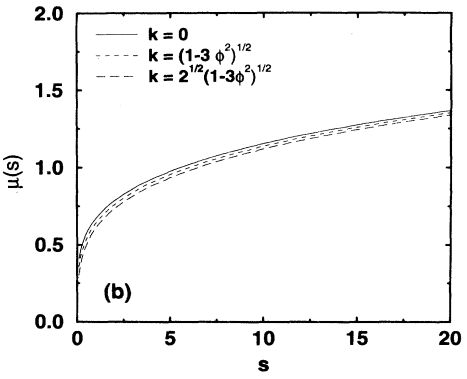

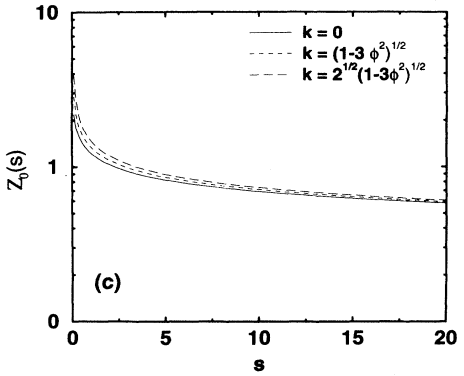

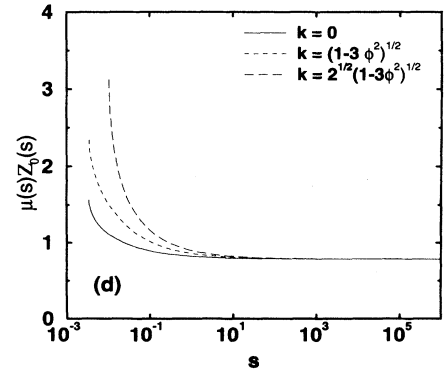

FIG. 9. Same as Fig. 7 but for $\phi_0 = 0.56$.

phase $\varphi(s)$ defined in Eq. (24) is close to zero, we have in Eq. (20) nearly a pure cosine function, and the zeros defined in Eq. (35) occur at

$$\mu(s)Z_0(s) = \frac{(2n+1)}{2}\pi \ , \quad n = 0, 1, \ldots \ , s \to 0 \qquad (38)$$

while for large s Eqs. (21), (31), and (32) imply $\Omega(s) \to 1$ and then

$$\mu(s)Z_0(s) = \frac{\pi}{4} + \frac{(2n+1)}{2}\pi \ , \quad n = 0, 1, \ldots \ . \qquad (39)$$

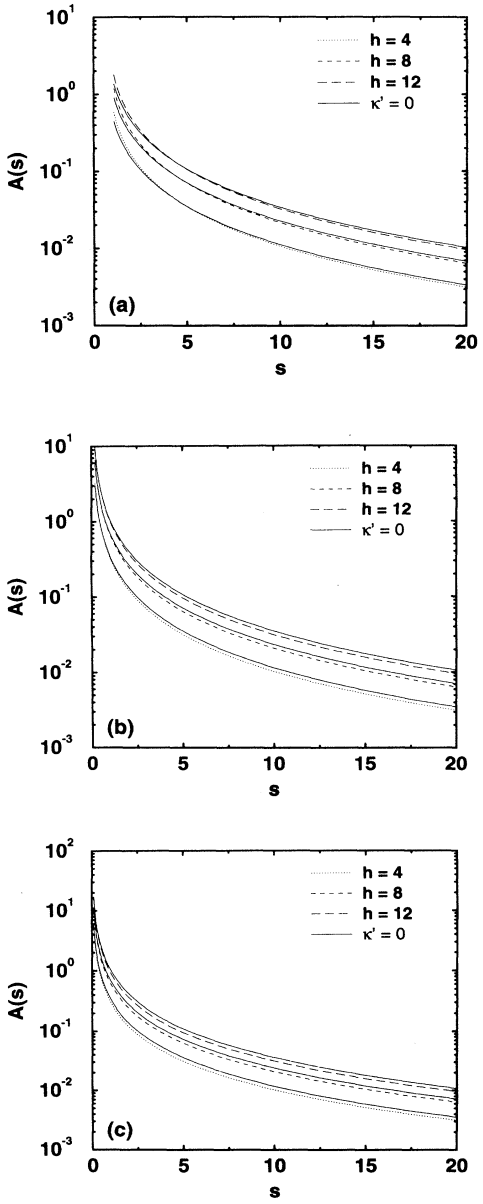

FIG. 10. Plot of the amplitude $A(s)$ versus scaled frequency s, for the case $\gamma = 4$, $g = -4$, $k_{\|} = 0$, $\phi_0 = 0$ (a), $\phi_0 = 0.47$ (b), and $\phi_0 = 0.56$ (c), for a variety of choices of the scaled surface field h, as indicated in the figure.

As an example for the spirit of this discussion, we present first some numerical examples for $V(Z, s)$ in the case $h_1 = 4$, $\gamma = 4$, $g = -4$, and $\phi_0 = 0$, for which a numerical solution of the full nonlinear equation was presented in Ref. [16] for several values of $k_{\|}$ and suitable values of s compatible with Eqs. (33) and (34). One sees that for s near s_0' and $k_{\|} = 0$ the damping of the concentration wave is rather small, one can resolve several oscillations with Z, while for large s the damping is fairly rapid [Fig. 4(a)]. But nevertheless the wavelength describing the oscillations of the function $V(Z, s)$ depends only little on s in this range.

Figures 5 and 6 show analogous results for a case just inside the spinodal, $\phi = 0.56$ (the spinodal is given by

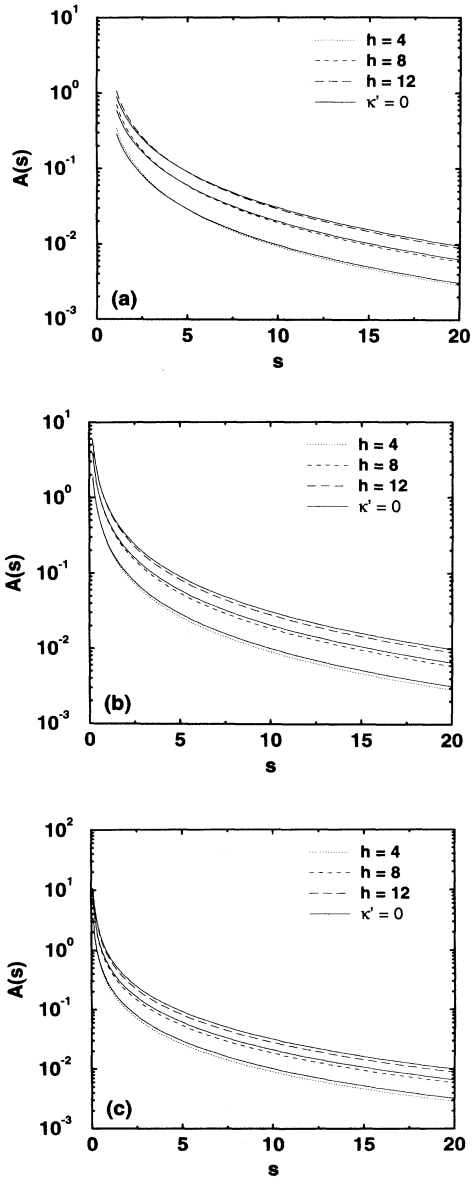

FIG. 11. Same as Fig. 10 but for $g = -8$ (where one is on the wet rather than nonwet side of the transition).

$1 - 3\phi_0^2 = 0$, i.e., $\phi_0 = \sqrt{3}^{-1} \approx 0.577$) and a case which is distinctly off critical but not yet very close to the spinodal, $\phi_0 = 0.47$. One can see that the characteristic linear dimension of the surface-enriched layer strongly increases as the spinodal is approached, while otherwise the qualitative characteristics of the behavior are still the same as in Fig. 4. Of course, the divergence of the critical wavelength of the linear theory of spinodal decomposition at the spinodal curve is a mean field artifact [24–34] and hence we do not expect much evidence for this critical increase of the linear dimension of the surface-enriched layer in real systems, apart from the case of polymer mixtures with very high molecular weight for which the spinodal becomes a precise meaning [30,31].

After having verified that the results of our treatment make physical sense—at least if we stay off the spinodal curve—we discuss now the frequency dependence of the various quantities of our treatment in more detail. Figures 7–9 show the decay constant $\nu(s)$, wavelength $\mu(s)$, and the position $Z_0(s)$ of the zeros for the three cases $\phi_0 = 0$, $\phi_0 = 0.47$, and $\phi_0 = 0.56$ studied above. Remember that these results are completely independent of the boundary condition at the surface—the latter enters only via the amplitude function $A(s)$. Of course, in the time domain we then have a convolution of these various dependencies through the inverse Laplace transform.

We recognize that $\nu(s)$ and $\mu(s)$ are always monotonically increasing functions of s. For $k_{\|} = 0$ and $\phi_0 = 0$ the s dependence of $\mu(s)$ is rather weak, while $\nu(s)$ increases much more strongly. This fact is responsible for the observation that the behavior at the smallest admissible frequencies dominates the oscillations in the profile. While for $\phi_0 = 0$ the dependence on $k_{\|}$ is very pronounced, for ϕ_0 near the spinodal it is rather weak. Note that the choices of $k_{\|}$ correspond to the wavelength of maximum growth and to the critical wavelength ($k_{\|}^{\max} = \sqrt{1 - 3\phi_0^2} = k_{\|}^c/\sqrt{2}$) for spinodal decomposition in the bulk.

Since the position of the first zero $Z_0(s)|_{n=0}$ decreases rather rapidly from its initial value $\pi/2 (s \to 0)$ to smaller values with increasing s, the prediction of the zeros of $\delta\phi(Z,t)$ needs the inverse Laplace transform of our results and hence is a rather subtle matter. For the arrows in Fig. 2(b) we have used Eq. (39) as a simple approximation.

Finally, Figs. 10 and 11 study the effect of the boundary condition at the surface, which enter via $A(s)$. One can see that $A(s)$ decreases rapidly with increasing scaled frequency s. Thus it is clear that the frequencies at the lower cutoff [s_0 or s_0', Eqs. (33) and (34)] will dominate in the Laplace transform. Hence the time scale for the growth of the profile in Fig. 2(b), in the initial stages where the linear theory is supposed to be valid, is of the order of $(s_0')^{-1} = (1 - 3\phi_0^2)^{-1}$. It is also remarkable that $A(s)$ changes only rather little if the higher order term in the boundary condition Eq. (15) is neglected (setting formally $\kappa' = 0$ there and in the following). This observation implies that there is only a small quantitative difference between the solution of the truncated equation [where the second term with the derivative proportional to κ' in Eq. (15) is omitted from the outset] and the full equation. Thus one can understand now why the treatments based on the full boundary condition [13,16,17] and the truncated one [14,15] are qualitatively very similar.

IV. DISCUSSION AND CONCLUSIONS

In this paper, we have presented an extension of the linearized theory of spinodal decomposition due to Cahn and Hilliard [20] to include the effect of free surfaces. We assume, however, that the effect of the surface is strictly local, disregarding possible effects due to long range forces, and hence the surface effects come in only through the effect of boundary conditions on the Cahn-Hilliard differential equations. There are two such boundary conditions, both of which have a clear physical interpretation: Eq. (3) [or Eq. (16), respectively] says that the concentration current across the boundary is zero; the other one [Eqs. (2) or (15), respectively] describe the relaxation of the local order parameter at the surface, responding to the surface field and change of interactions at the surface, etc. We have also examined the effect of working with an approximate boundary condition rather than the exact one, as is sometimes done [14,15], and have found that in typical cases it makes little difference.

Our results reiterate the finding of previous numerical work [16,17], that during the initial stages it makes little difference whether one considers conditions of nonwet or wet static equilibrium at the surface. The interpretation of this finding is that the possible growth of a wetting layer is such a slow process that it does not interfere with the much faster growth of a surface-directed concentration wave. Typically [cf. Figs. 4(a), 5(a), and 6(a)] the amplitude of the damped oscillatory concentration profile is rather large at the surface, for the dominating frequency (s_0 or s_0', respectively), and hence an enrichment layer at the surface forms rapidly, irrespective of the state in the surface phase diagram (Fig. 3). The length scale of this enrichment zone is given entirely in terms of bulk properties, see Eqs. (31) and (39); the boundary conditions enter solely via the amplitude $A(s)$, Eq. (23). Of course, this exact factorization of boundary effects and effects dominated by bulk properties is exactly true only in the linearized theory and in the frequency domain; the Laplace transform to Eq. (13) should be evaluated to transform our results to the time domain, but since this is no longer analytically possible this numerically cumbersome step has been avoided. But a comparison to the numerical data [Fig. 2(b)] suggests that this conclusion can at least approximately be carried over to the final solution of the full nonlinear equation as well.

The fact that the scale of the oscillations of the concentration profile near the surface is basically set by the wavelength of spinodal decomposition in the bulk is recognized when we use $s = s_0'$ for $k_{\|} = 0$ in Eq. (31), which yields

$$\mu^2(s_0') = (1 - 3\phi_0^2). \tag{40}$$

From Eqs. (7) and (8) we see that the wave num-

ber k_{max} of a maximum growth in the bulk also is given by $k^2_{max} = a/2 = 1 - 3\phi_0^2$ in our normalization ($k_{max} = 2\pi/\lambda_m$, cf. Fig. 1). Thus, the wavelength of maximal growth, dominating spinodal decomposition in the bulk, appears to control also the surface behavior. Consequently, approaching the spinodal one can see a divergence of this length, which is quite obvious from the profiles [Figs. 4(a), 5(a), and 6(a)]. It is quite clear that this singular behavior at the spinodal $\{\phi_{0s} = 1/\sqrt{3}$, both $\mu^2(s_0')$ and k^2_{max} vanish when $\phi_0 \to \phi_0^s\}$ will be wiped out due to the combined effect of nonlinearities and statistical fluctuations [28–34]. Numerical studies checking this behavior near the spinodal would be very desirable, as well as experiments on polymer mixtures with high molecular weight, where some remnants of this singular behavior might be detectable due to the mean field character of these systems [30,31].

We also emphasize that the decay constant $\nu(s)$ for s near s_0' always is of the same order as $\mu(s_0')$, since Eq. (32) implies for $k_{||} = 0$ and $s = s_0'$ that $\nu^2(s_0') = 0$, i.e., exactly at this boundary the wave would be undamped, but it is clear from Eq. (32)—and also evident from Figs. 6–8—that $\nu(s)$ increases rapidly to similar values as $\mu(s)$.

In conclusion, we have demonstrated here that the investigation of surface effects on spinodal decomposition would provide another means of testing the linearized theory of spinodal decomposition in the bulk, if the surface can actually be characterized by a short range perturbation as assumed here. We hope that our study will stimulate corresponding experiments to test these predictions.

ACKNOWLEDGMENTS

One of us (H.L.F.) acknowledges partial support from the National Science Foundation under NSF Grant No. DMR9023541, the Donors of the Petroleum Fund of the American Chemical Society, and the Deutsche Forschungsgemeinschaft (DFG) under Sonderforschungsbereich (SFB) 262/D2. P.N. acknowledges financial support from the Deutsche Forschungsgemeinschaft (Heisenberg Foundation). We are grateful to S. Puri and G. Krausch for stimulating discussions.

[1] R.A.L. Jones, L.J. Norton, E.J. Kramer, F.S. Bates, and P. Wiltzius, Phys. Rev. Lett. **66**, 1326 (1991).
[2] P. Wiltzius and A. Cumming, Phys. Rev. Lett. **66**, 3000 (1991).
[3] U. Steiner, E. Eiser, J. Klein, A. Budkowski, and L. J. Fetters, Science **258**, 1126 (1992).
[4] F. Bruder and R. Brenn, Phys. Rev. Lett. **69**, 624 (1992).
[5] H. Tanaka, Phys. Rev. Lett. **70**, 53 (1993).
[6] B.Q. Shi, C. Harrison, and A. Cumming, Phys. Rev. Lett. **70**, 206 (1993).
[7] G. Krausch, C.A. Dai, E.J. Kramer, J. Marko, and F.S. Bates, Macromolecules **26**, 5566 (1993).
[8] G. Krausch, E.J. Kramer, F.S. Bates, J.F. Marko, G. Brown, and A. Chakrabarti (unpublished).
[9] G. Krausch, C.A. Dai, E.J. Kramer, and F.S. Bates, Phys. Rev. Lett. **71**, 3669 (1993).
[10] U. Steiner, J. Klein, and L.J. Fetters, Phys. Rev. Lett. **72**, 1498 (1994).
[11] U. Steiner, E. Eiser, A. Budkowski, L.J. Fetters, and J. Klein, in *Ordering in Macromolecular Systems*, edited by A. Teramoto (Springer, Berlin, in press).
[12] G.M. Xiong and C.D. Gong, Phys. Rev. B **39**, 9384 (1989); R.C. Ball and R.H.L Essery, J. Phys. Condens. Matter **2**, 10 303 (1990).
[13] S. Puri and K. Binder, Phys. Rev. A **46**, R4487 (1992).
[14] G. Brown and A. Chakrabarti, Phys. Rev. A **46**, 4829 (1992).
[15] J.F. Marko, Phys. Rev. E **48**, 2861 (1993).
[16] S. Puri and K. Binder, Phys. Rev. E **49**, 5359 (1994).
[17] S. Puri and K. Binder, J. Stat. Phys. **77**, 145 (1994).
[18] C. Sagui, A.M. Somoza, C. Roland, and R.C. Desai, J. Phys. A **26**, L1163 (1993).
[19] Y. Oono and S. Puri, Phys. Rev. Lett. **58**, 836 (1987); Phys. Rev. A **38**, 434 (1988).
[20] J.W. Cahn and J.E. Hilliard, J. Chem. Phys. **28**, 258 (1958); J.W. Cahn, Acta Metall. **9**, 795 (1961).
[21] K. Binder and H.L. Frisch, Z. Phys. B **84**, 403 (1991).
[22] H.W. Diehl and H.-K. Janssen, Phys. Rev. A **45**, 7145 (1992); see also H.W. Diehl, Phys. Rev. B **49**, (1994).
[23] R. Lipowsky and D.A. Huse, Phys. Rev. Lett. **52** 353 (1986).
[24] For reviews see J.D. Gunton, M. San Miguel and P.S. Sahni, in *Phase Transitions and Critical Phenomena, Vol. 8*, edited by C. Domb and J.L. Lebowitz (Academic Press, London, 1983), p. 267, and Refs. [25–27].
[25] *Dynamics of Ordering Processes in Condensed Matter*, edited by S. Komura and H. Furukawa (Plenum Press, New York, 1988).
[26] K. Binder, in *Materials Science and Technology, Vol. 5: Transformations in Materials*, edited by R.W. Cahn, P. Haasen, and E.J. Kramer (VCH, Weinheim, 1991), p. 405.
[27] G. Kostorz (unpublished); Phys. Scr. **T49**, 636 (1993).
[28] K. Binder, Phys. Rev. B **8**, 3423 (1973).
[29] J.S. Langer, Physica **73**, 61 (1974).
[30] K. Binder, J. Chem. Phys. **79**, 6387 (1983); Phys. Rev. A **29**, 341 (1984).
[31] K. Binder, Physica **140A**, 35 (1986).
[32] H.-O. Carmesin, D.W. Heermann, and K. Binder, Z. Phys. B **65**, 89 (1986).
[33] A.B. Bortz, M.H. Kalos, J.L. Lebowitz, and M.A. Zendyas, Phys. Rev. B **10**, 535 (1974); J. Marro, A.B. Bortz, M.H. Kalos, and J.L. Lebowitz, *ibid.* **12**, 2000 (1975).
[34] J.S. Langer, M. Baron, and H.D. Miller, Phys. Rev. A **11**, 1417 (1975).
[35] F.S. Bates and P. Wiltzius, J. Chem. Phys. **91**, 3258 (1989).
[36] For a recent review, see T. Hashimoto, in *Materials Science and Technology, Vol. 12: Structure and Properties*

of Polymers, edited by R.W. Cahn, P. Haasen, and E.J. Kramer (VCH, Weinheim, 1993), p. 251.

[37] K. Kawasaki, in *Phase Transitions and Critical Phenomena, Vol. 2*, edited by C. Domb and M.S. Green (Academic, London, 1972), Chap. 11.

[38] For a review, see S. Dietrich, in *Phase Transitions and Critical Phenomena, Vol. 12*, edited by C. Domb and J.L. Lebowitz (Academic, London, 1988), p. 1.

[39] I. Schmidt and K. Binder, Z. Phys. B **67**, 369 (1987).

[40] S. Puri and K. Binder, Z. Phys. B **86**, 263 (1992).